

Observations and models of slow solar wind with Mg^{9+} ions in quiescent streamers

L. Ofman^{1,2,3}, L. Abbo⁴, S. Giordano⁴

Received _____; accepted _____

¹Catholic University of America, Washington, DC 20064

²NASA Goddard Space Flight Center, Code 671, Greenbelt, MD 20771

³Visiting Associate Professor, Department of Geophysics and Planetary Sciences, Tel Aviv University, Tel Aviv 69978, Israel

⁴INAF, Astrophysical Observatory of Turin, Italy

ABSTRACT

Quiescent streamers are characterized by a peculiar UV signature as pointed out by the results from the observations of the Ultraviolet and Coronagraph Spectrometer (UVCS) on board SOHO: the intensity of heavy ion emission lines (such as O VI) show dimmer core relative to the edges. Previous models show that the structure of the heavy ion streamer emission relates to the acceleration regions of the slow solar wind at streamer legs and to gravitational settling processes in the streamer core. Observations of Mg⁹⁺ ion EUV emission in coronal streamers at solar minimum were first reported by the UVCS instrument. The Mg X 625Å emission is an order of magnitude smaller than the O VI 1032 Å emission, requiring longer exposures to obtain statistically significant results. Here, Mg X coronal observations are analyzed and compared, for the first time, with the solar minimum streamer structure in hydrogen and O VI emissions. We employ the 2.5D three-fluid model, developed previously to study the properties of O⁵⁺ ions in streamers, and calculate for the first time the density, temperature, and outflow structure of Mg⁹⁺ ions in the solar minimum streamer. The Mg⁹⁺ ions are heated by an empirical radial heating function constrained by observations of the kinetic ion temperature obtained from Mg X emission line profiles. The detailed structure of Mg⁹⁺ density, temperature, and outflow speed is determined by the Coulomb momentum and energy exchange as well as electromagnetic interactions with electrons and protons in the three-fluid model of the streamer. The results of the model are in good qualitative agreement with observations, and provide insights on the possible link between the magnetic structure of the streamer, slow solar wind sources, and relative abundances of heavy ions.

1. Introduction

One of the main results obtained from the observations performed by the Ultraviolet and Coronagraph Spectrometer (UVCS) on board SOHO was the dramatic difference in the line profiles and the emission variation in latitude across quiescent streamers of heavy ions such as O VI 1032 Å compared to the H I Ly α 1216 Å emission (e.g., Kohl et al. 1997; Raymond et al. 1997; Noci et al. 1997; Kohl et al. 1999; Marocchi et al. 2001; Zangrilli et al. 2001; Strachan et al. 2002; Uzzo et al. 2003, 2004; Vásquez & Raymond 2005; Uzzo et al. 2006, 2007; Akinari 2007). This variation in emission was attributed to the variation in heavy ion relative abundance across streamers and to slow solar wind acceleration regions in several numerical multi-fluid models (Ofman 2000, 2004; Chen & Li 2004; Morgan et al. 2008; Ofman et al. 2011). Note, that modeling the self consistent interaction between heavy ions, protons, and electrons in coronal streamers requires multi-fluid models as the next level of physical approximation beyond a single-fluid MHD. In these models the electrons, protons, and heavy ions are described as electromagnetically, and collisionally interacting charged fluids with overall quasi-neutrality. The electron inertia is usually neglected compared to the proton inertia, and the electron momentum equation is used to solve for the electric field (generalized Ohm’s law). Separate coupled continuity, momentum, and energy equations are solved for each particle species together with Maxwell’s equations.

Recently, Ofman et al. (2011) used the 2.5D (azimuthally symmetric) 3-fluid model to study the UV emission from H I Ly α 1216 Å and O VI 1032 Å spectral lines in a streamer belt during solar minimum (CR 1913) observed with UVCS/SOHO. Dipole magnetic field configuration was included in the initial state and preferential heating for O⁵⁺ ions was considered with coupled polytropic energy equations for electrons protons and ions. The model relaxed to a steady state with a coronal streamer belt and a slow solar wind that included the heavy ions. The results of the model provide information on the slow solar

wind acceleration regions in the streamer belt, the interactions between the species, and the velocity, density, and temperature variations of the electrons, protons, and O^{5+} ions in the streamers. The model results were used to synthesize UV observables in the above spectral lines and very good agreement was found with UVCS observations. Abbo et al. (2010b) used the results of single-fluid MHD mode to determine the edges of streamers and compared the results with the UVCS observational of O VI emission variation across a streamer. First detailed comparisons between O VI emission in streamers and 3-fluid model results were done by Ofman (2000, 2004). Recently, a preliminary comparison to multi-fluid model was performed by Abbo et al. (2010a) that was extended in a detailed study by Ofman et al. (2011). Since the interactions between the various heavy ion species as well as their effect on protons and electrons is negligible due to their low relative abundances, one has the freedom to choose any single minor heavy ion species in the three-fluid model calculations. Here, we extend our previous studies by introducing Mg^{9+} as the heavy ion species, and investigate the details of the ion streamer density, temperature, velocity, and UV emission. This is the first detailed observational study of streamer emission and images in Mg x 625 Å, and the first detailed 2.5D three-fluid modeling of streamers that include Mg^{9+} ions in addition to protons and electrons. In particular, the aim of this study is to compare the observed radial and latitudinal emission profiles with the expected ones from multi-fluid MHD model of coronal streamer as seen in H I Ly α and in Mg x to validate the model results and better understand the origin of the slow solar wind.

2. Quiescent Streamers Observations in Mg x 625 Å

The doublet of UV coronal emission lines from Mg^{9+} at 609.76 Å and 624.93 Å, here called Mg x 610 Å and Mg x 625 Å can be detected by UVCS spectra-coronagraph at the second order in the channel optimized for O VI lines at 1032 Å and 1037 Å, that includes

longer wavelength from its redundant optical path. The expected most intense Mg x 610 Å emission falls on the red wing of the very bright and wide H I Ly α at 1215.67 Å, therefore, the spectral analysis is more difficult due to lower signal to noise ratio than for Mg x 625 Å which falls about 30 Å away from the H I line. Thus, we focus on Mg x 625 Å emission and in particular on the study of the quiescent coronal streamers that show the typical intensity dimming in the central region of the streamers as observed in O VI lines, in order to answer the question whether this dimming is present in emission lines from heavier ions, such as Mg x. Multi-fluid models have shown that the density structure of the heavy ions are closely related to the structure of the slow solar wind in streamers (e.g., Ofman 2000, 2004). The quiescent streamers are well defined at the minimum of solar activity at the equatorial latitudes, in particular at the minimum of cycle 22 (1996–1997) the streamer belt was very stable and could be modeled reasonably well by 2.5D model with initial dipole magnetic field (e.g., Ofman & Kramar 2010; Ofman et al. 2011).

Because of the low Magnesium abundance in the solar corona ($\simeq 4 \times 10^{-5}$ relative to Hydrogen for all ionization states) and the reduced second order lines instrument efficiency, the photon count rates from Mg x lines are low, therefore to reach a good statistics, a very long exposure time is required. Alternatively, multiple observations of streamers with shorter exposures are combined to reconstruct an averaged Mg x 625 Å emission radial and latitudinal profiles.

Almost daily observations of Mg x 625 Å line were performed with UVCS from 1997 July 31 to November 25. In that period we identified the long-lived quiescent streamers by looking at LASCO C2 observations of west and east limbs. Next, we analyzed the corresponding intensity profiles of H I Ly α and O VI 1032 Å in order to identify the cases of evident core-dimming in O VI. Thus, for these streamers, we consider the Mg x 625 Å spectra to determine the intensity profiles.

A sample of the streamer observations considered in the study is shown in the left panel of Figure 1, where the background image is the visible light scattered by coronal electrons from LASCO C2 observations, and the vertical strip is the O VI 1032 Å line intensity detected by UVCS. The data were obtained on August 22, 1997. The right panel of Figure 1 shows the latitudinal intensity profiles at 1.63 R_⊙ of H I Ly α (blue), O VI 1032 Å (black) and Mg X 625 Å (red) spectral lines. The depletion in O VI emission at the center of the streamer is evident and there is indication of the core-dimming also in Mg X emission line, although of lower magnitude.

The Mg X 625 Å line intensity profile as a function of the radial distance has been derived using UVCS data from August 23 and September 26, 1997 that were obtained up to heliocentric distances of 2.75 and 2.28 R_⊙, respectively. In the latter case we were able to reconstruct the Mg X coronal image from a streamer scan that clearly shows the presence of a core-dimming from Mg⁹⁺ ion emission. The Mg X core-dimming is less pronounced in comparison with the dimming seen in O⁵⁺ ion emission (Figure 2). We determine the width of Mg X spectral line by analyzing observations with narrow slits. There are only few UVCS streamer observations of Mg X 625 Å line with narrow slit during the solar minimum; moreover, these observations do not provide good spatial resolution data, because of the narrow slit and resulting low count rate. Therefore, it is difficult to determine the spectral parameters in streamer core and legs, separately. The values averaged over about 500'' around the streamer axis are reported in Table 1 where the line widths are given in terms of most probable velocity ($V_{1/e}$) and of kinetic temperature, $T_{k,i}$, both for Mg X and O VI lines. Note that the relation between $T_{k,i}$ and $V_{1/e}$ is given by $T_{k,i} = \frac{A_i m_p}{2k_B} V_{1/e}^2$, where A_i is the atomic mass number of the ions, m_p is the proton mass, and k_B is Boltzmann's constant.

In quiescent streamer at solar minimum we find that $V_{1/e}$ of Mg⁹⁺ ions is comparable or

slightly larger than that of O^{5+} ions, that is $V_{1/e,MgX} \geq V_{1/e,OVI}$ and the kinetic temperature of Mg^{9+} ions is much larger than that of O^{5+} ions. While the mass ratio of Mg^{9+} ions and O^{5+} ions is 1.5, the kinetic temperature ratio is on average about a factor of two (i.e., $T_{k,MgX}/T_{k,OVI} \sim 2$, as evident in Table 1). The high ion temperatures suggest more than mass proportional heating, in agreement with previous studies in coronal holes (e.g., Kohl et al. 1999; Cranmer et al. 1999). However, the temperature ratio between the two ions in streamers has the opposite trend compared to the observations in coronal holes that find higher O^{5+} temperatures than Mg^{9+} temperatures (e.g. Kohl et al. 1999; Esser et al. 1999).

3. Three-fluid model: boundary conditions and numerical results

We employ the 2.5D three-fluid model used recently to model coronal streamers with O^{5+} ions at solar minimum (see, Ofman et al. 2011, for further details of the model), with brief description of the model provided below. The streamer calculation is initialized with a potential dipole magnetic field normalized by $B_0 = 7$ G, initial temperature $T_0 = 1.6MK$, and normalization density $n_0 = 5 \times 10^8 \text{ cm}^{-3}$, and the corresponding Alfvén speed $V_A = 683 \text{ km s}^{-1}$. These values are used to calculate the solar wind velocity with the isothermal Parker’s solution as the initial state for the three-fluid model. A polytropic energy equation with $\gamma = 1.05$ is solved for each particle species with the addition of collisional energy exchange terms, and with observationally constrained empirical heating term for Mg^{9+} ions to model their preferential heating (see below). The mass continuity and momentum equations are solved for protons and heavy ions, while charged neutrality is used to obtain the electron density. The neglect of electron inertia is used obtaining the generalized Ohm’s law, and the electric field is used in the momentum equations that include Coulomb friction terms between the various species. The electron velocity is used in the induction equation

and the gyro-motions of the ion fluids are neglected in the low-frequency (MHD) limit. The boundary conditions are open at the outer boundary, and fixed field at the lower boundary, with extrapolated density, temperature, and velocity (based on the method described in Steinolfson & Nakagawa (1976)). The resolution is 320 grid cells in θ in the (approximate) range 0 to π , and 1028 in r in the range $(1, 8) R_{\odot}$.

We modify the model to study the dynamics of Mg^{9+} ions by adopting the parameters for the Mg^{9+} ions as the third fluid; i.e., the charge $Z = 9$ and atomic mass to $A = 24$, and we use the relative abundance of $n_{\text{Mg}^{9+},0} = 5 \times 10^{-6}$ (Mazzotta et al. 1998) at $r = 1R_{\odot}$ of the model. Note, that as in previous three-fluid models we assume that the ionization state remains fixed, i.e., the ionization and recombination of Mg^{9+} is at steady state, even though the electron temperature is not constant. This is justified by the result that at steady state the closed field region of a quiescent streamer is in hydrostatic equilibrium, with (nearly) constant electron temperature (e.g., Pneuman & Kopp 1971), while in open field region the ionization state of Mg^{9+} ions becomes frozen-in within $1.5R_{\odot}$ when ion lifetime is compared to the solar wind expansion time (e.g., Withbroe et al. 1982; Esser et al. 1999). The initial Mg^{9+} relative abundance is uniform in the computational domain. The initial Mg^{9+} temperature $T_{i,0} = 42$ MK, and the initial electron and proton temperatures $T_{e,0} = T_{p,0} = 1.6$ MK are uniform. Note, that $T_{i,0}$ is taken to be large so that the initial hydrostatic Mg^{9+} ion density does not decrease to zero at the top of the streamer. However, as the solution evolves to steady state, T_i decreases rapidly and the density structure coupled to the protons and electrons becomes more realistic. We have iterated on the value of $T_{i,0}$ to provide the best match with the observed Mg x emission in the streamer. In addition, we study the parameters of the ion empirical heating function given by

$$S_i = S_{i0}(r - 1)e^{-(r-1)/\lambda_{i0}}, \quad (1)$$

where the parameters S_{i0} and λ_{i0} determine the magnitude and the decrease of the heating

rate with distance, r . The heating function parameters are adjusted to match the $T_{k,MgX}$ values in the center of the streamer at the steady state determined from the line profiles given in Table 1. We found that $S_{i0} \approx 7.5 \times 10^2$ and $\lambda_{i0} = 0.225R_{\odot}$ provide the best match with observations for Mg^{9+} ion temperature structure in the present model. It is interesting to note that in Ofman et al. (2011) the value of S_{i0} for O^{5+} ions was ~ 26 times smaller, and the value of λ_{i0} was a factor of two larger than in the present study. The three-fluid model is evolved until the streamer solution reaches a (quasi-) steady state, with the typical closed field and open field region structures separated by a current sheet. We use the term quasi-steady state since after the rapid evolution stage the streamer still evolves slowly at this stage. The Mg^{9+} temperature decreases quickly to much lower values while the electron and proton temperatures do not strongly vary as the solution reaches the steady state. Note, that the model is aimed at studying the slow solar wind in the streamer, and does not include the additional momentum input in open field regions required for fast solar wind solutions.

In Figure 3 the densities of protons and Mg^{9+} ions and the corresponding radial outflow velocities of the streamer in steady state at $t = 98.1\tau_A$ (about 30 hours) are shown. The proton density shows an increase in the closed field region where the plasma is confined and compressed by the Lorentz force produced by the current-sheet that separates the closed and open field region (i.e., pressure balance, see Pneuman & Kopp (1971)). However, the Mg^{9+} ion density shows the typical darkening in the closed field region of the streamer, consistent with previous model and observations of O^{5+} ions, and consistent with the observed Mg^{9+} emission shown in Figure 2c. The model shows (examining the quantitative effects of the various terms) that this structure of Mg^{9+} is the result of gravitational settling in the closed field region of the heavy Mg^{9+} ions, and the coupling between the outflowing protons and Mg^{9+} ions due to the Coulomb friction in the open field region, resulting in increase of the relative Mg^{9+} ion abundance compared to the abundance in the closed field

region. The gravitational settling is limited by the quasi-neutrality of the plasma that increases the effective scale-height of Mg^{9+} ions, consistent with previous results (Lenz 2004; Ofman et al. 2011). Temporal evolution of Mg^{9+} density structure and the formation of the density dip in the core of the streamers are evident from the enclosed animation of the Mg^{9+} ion density. However, the details of the evolution and the time scale are the results of initial conditions of the idealized model, and we should expect only qualitative agreement of the evolution with observations.

The kinetic temperatures of electrons, protons, and Mg^{9+} ions calculated with the three-fluid model at $t = 98.1\tau_A$ are shown in Figure 4. It is evident that the electron and proton temperature structure is similar, peaking in the closed field region of the streamer at $T = 1.6MK$, consistent with observations of a coronal streamer at solar minimum and with previous three-fluid model (e.g. Ofman et al. 2011). The electron and proton temperatures are nearly constant in the closed field regions. This is the result of hydrostatic equilibrium in forming at the steady state of the quiescent streamer (see, e.g. Pneuman & Kopp 1971). There is only small variation of T_e and T_p due to the confinement pressure exerted by the Lorentz force from the current sheet surrounding the streamer. The nearly steady T_e and T_p in the core of quiescent streamer is in agreement with observations (e.g. Strachan et al. 2002; Antonucci et al. 2005; Uzzo et al. 2007).

However, the temperature structure of Mg^{9+} ions show very different structure. The temperature structure is the result of the application of the simple spherically symmetric, radially dependent heating function (Equation 1) in the three-fluid model, combined with the effects of the magnetic structure of the streamer, and the collisional (Coulomb) coupling between the ions, protons, and electrons. In particular, in the closed field regions the collisional thermal energy exchange between the heated Mg^{9+} ions and the cooler protons and electrons leads to lower temperature of the Mg^{9+} ions compared to their temperature

outside the closed field region of the streamer. This temperature structure of the Mg^{9+} ions is consistent with UVCS observations and model results for O^{5+} ions (e.g., Ofman et al. 2011). Thus, although the simple heating function provides only radial dependence of the heating, the complex coupling between the three-fluids, the magnetic field, and the outflows leads to the structure of the latitudinal dependence of the Mg^{9+} ion temperature.

The details of the outflow speed, density, and temperature in a radial cut through the center of the solar minimum streamer are shown in Figure 5. In Figure 5a it is evident that the radial outflow speed is nearly zero in the closed field region of the streamer ($r < 4R_{\odot}$) consistent with previous observations of O^{5+} ions (e.g., Strachan et al. 2002). In the stalk of the streamer the outflow speed of protons and Mg^{9+} ions is similar, reaching $\sim 100 \text{ km s}^{-1}$ at $r = 8R_{\odot}$. The normalized density of both, protons and Mg^{9+} ions decreases rapidly with height, as expected in the solar wind streamer, shown in Figure 5b. It is interesting to note, that the Mg^{9+} ion density shows clear transition between the closed field region, with rapid decrease of their density with height, and the stalk of streamer, where the variation of the Mg^{9+} density is small, due to coupling with outflowing protons. The corresponding kinetic temperatures obtained from the model are shown in Figure 5c. It is evident that the Mg^{9+} ion temperature shows rapid increase reaching 7.5 MK at about $1.6 R_{\odot}$, and then decreases up to $3.5 R_{\odot}$, matching the proton and electron temperature outside the streamer. The kinetic temperature with error bars of Mg^{9+} ions obtained from observations are shown, and the model results produce good agreement.

The cross-section of the streamer in the latitudinal (θ) direction at $r = 1.61 R_{\odot}$ is shown in Figure 6. The outflow speed is small inside the streamer, consistent with the previous results. The normalized density (to the value at $\theta = 0$) of protons and Mg^{9+} ions shows opposite variation inside the closed field region of the streamer compared to the open field region outside. It is evident that the protons density is nearly 3 times larger inside

the streamer, compared to the density outside at this height. The Mg^{9+} ion density in the core of the streamer is about half the density outside at this height. The temperature of protons and electrons inside the streamer is increased by about 50% compared to the outside temperature, while the Mg^{9+} ion temperature is lower by a factor of ~ 2.8 compared to the temperature outside the closed field region of the streamer at this height, even though the heating function is spherically symmetric. The agreement between the model and the observed Mg^{9+} kinetic temperature in the center of the streamer is evident. The temperature increase outside the streamer is consistent with past observations of emission line broadening of Mg x in coronal holes (Kohl et al. 1999). The nearly steady radial dependence of T_e and T_p in the core of the quiescent streamer is evident.

The densities, temperatures, and velocities of the coronal electrons, protons, and Mg^{9+} ions obtained from the 2.5D three-fluid model are used to compute the expected intensity from H I Ly α and Mg x 625 Å spectral lines, employing the same method as described in Section 4.2 in Ofman et al. (2011). In our computation of the radiative component, we assumed uniformly bright exciting radiation coming from the solar disk, in particular for H I Ly α we adopted the SUMER profile observed at solar minimum in 1996 July (Lemaire et al. 2002) and for Mg x 625 Å the intensity reported by Andretta et al. (2012), and the line width by Landini & Monsignori Fossi (1990). For the collisional component, we consider the ionization equilibrium by Mazzotta et al. (1998) for H I atoms and by Arnaud & Rothenflug (1985) for Mg^{9+} ions. The integration along the line-of-sight has been performed by assuming a cylindrical (azimuthal) symmetry and the derived intensity maps are shown in Figure 7 in normalized units, compare well with the images in Ly α and Mg x line intensities shown in Figure 2 obtained from the UVCS observations (rotated by 90°). In the bottom panel, the latitudinal variation of the normalized intensities are shown for H I Ly α (solid curve) and for Mg x (dotted) lines at $1.63 R_\odot$, and compare well with the variation shown in the right panel of Figure 1. The normalized intensity of O VI

computed in Ofman et al. (2011) is also shown for comparison. Moreover, the radial profiles of H I Ly α and Mg X intensities averaged over the entire streamer region are shown in Figure 8. It is evident that the values computed from the model (solid lines) and the values obtained from the UVCS observations on August 23, 1997 (points and dashed lines) are in very good agreement.

4. Discussion and Conclusions

The origin of the slow solar wind has been associated with streamers in the past. However, the details of the slow solar wind acceleration process and the outflow regions are poorly known. Past UVCS observations of O VI ion emission and models of quiescent streamers show that the core of the streamer is characterized by lower relative abundance of the O⁵⁺ ions, and the legs of the streamers show increased relative ion abundance due to collisional interaction (Coulomb friction) with outflowing protons and electrons. It was suggested in the past (e.g. Raymond et al. 1997; Noci et al. 1997; Ofman 2000) that O⁵⁺ ion emission observations can be used as the diagnostic of the slow solar wind acceleration regions in coronal magnetic streamer legs, and the closed magnetic field regions in the quiescent streamer cores due to gravitational settling. Here we show for the first time using observations and detail modeling that these properties hold as well for Mg⁹⁺ ions and therefore are expected for other heavy ions in quiescent streamers not yet observed spectroscopically in streamers.

In the present study we analyze UVCS observations of Mg⁹⁺ EUV emission in the solar minimum streamer, and compare, for the first time, with hydrogen and O⁵⁺ intensities. Both heavy ion emissions are significantly different in structure from the H I Ly α emission, showing opposite dependence on latitude. In particular, we find that a streamer core dimming is visible both in O VI and in Mg X lines, although it is less prominent in Mg X.

We have derived the observed emission line widths at the center of the streamer to calculate the $V_{1/e}$ velocity and the corresponding kinetic temperature, $T_{k,i}$, of the Mg^{9+} ions. We find that in quiescent streamer at solar minimum, the $1/e$ velocity of Mg^{9+} ions is comparable or slightly larger than that of O^{5+} ions, that is $V_{1/e,\text{MgX}} \geq V_{1/e,\text{OVI}}$, and that $T_{k,\text{MgX}} \approx 2T_{k,\text{OVI}}$ indicating more than mass proportional heavy ion heating.

The three-fluid model developed to study the structure and dynamics of O^{5+} ions has been adapted for the present study of Mg^{9+} ions. The model shows that preferential and more than mass-proportional heating of the heavy ions (compared to protons and electrons) is required in order to reproduce the observed kinetic temperatures of the ions. Interestingly, only radial variation of the empirical ion heating function needs to be specified, while the three-fluid model produces the two-dimensional Mg^{9+} streamer temperature and density structure with good qualitative agreement with the available observations. We found from the three-fluid model that compared to O^{5+} the required heating per particle of Mg^{9+} is significantly larger and must be deposited closer to the Sun to match observations. The higher kinetic temperature of Mg^{9+} ions outside the streamer is consistent with the higher temperature of Mg^{9+} deduced in coronal holes (Kohl et al. 1999). The model also provides details on the density, temperature and outflow structure of Mg^{9+} ions in the solar minimum streamer not available from observations with present instruments (such as the separation between the core and the legs of the streamer). The output of the model was used to compute the expected H I Ly α and Mg X emission maps and the parameters of the model were iterated to optimized the agreement with observations. Good agreement was found for the radial profiles of the intensities, the core dimming of Mg X and the temperature profiles of the ions. We find that the effects of gravitational settling in the quiescent streamer core characterized by close magnetic field, and the Coulomb friction with the outflowing bulk solar wind in open field regions are the dominant processes that affect their relative abundance variation and outflow properties of Mg^{9+} ions.

LO would like to acknowledge support by NSF grant AGS-1059838 and NASA grant NNX10AC56G. UVCS is a joint project of NASA, the Agenzia Spaziale Italiana (ASI), and the Swiss Founding Agencies. LA has been funded through contract I/023/09/0 and I/013/12/0 between the National Institute for Astrophysics (INAF) and the Agenzia Spaziale Italiana (ASI).

REFERENCES

- Abbo, L., Antonucci, E., Mikić, Z., Linker, J. A., Riley, P., & Lionello, R. 2010a, *Advances in Space Research*, 46, 1400
- Abbo, L., Ofman, L., & Giordano, S. 2010b, *Twelfth International Solar Wind Conference*, ed. M. Maksimovic et al. (Melville, NY: AIP), 1216, 387
- Akinari, N. 2007, *ApJ*, 668, 1196
- Andretta, V., Telloni, D., & Del Zanna, G. 2012, *Sol. Phys.*, 279, 53
- Antonucci, E., Abbo, L., & Doderò, M. A. 2005, *A&A*, 435, 699
- Arnaud, M., & Rothenflug, R. 1985, *A&AS*, 60, 425
- Chen, Y., & Li, X. 2004, *ApJ*, 609, L41
- Cranmer, S. R., Field, G. B., & Kohl, J. L. 1999, *ApJ*, 518, 937
- Esser, R., Fineschi, S., Dobrzycka, D., Habbal, S. R., Edgar, R. J., Raymond, J. C., Kohl, J. L., & Guhathakurta, M. 1999, *ApJ*, 510, L63
- Kohl, J. L., Fineschi, S., Esser, R., Ciaravella, A., Cranmer, S. R., Gardner, L. D., Suleiman, R., Noci, G., & Modigliani, A. 1999, *Space Science Reviews*, 87, 233
- Kohl, J. L., Noci, G., Antonucci, E., Tondello, G., Huber, M. C. E., Gardner, L. D., Nicolosi, P., Strachan, L., Fineschi, S., Raymond, J. C., Romoli, M., Spadaro, D., Panasyuk, A., Siegmund, O. H. W., Benna, C., Ciaravella, A., Cranmer, S. R., Giordano, S., Karovska, M., Martin, R., Michels, J., Modigliani, A., Naletto, G., Pernechele, C., Poletto, G., & Smith, P. L. 1997, *Sol. Phys.*, 175, 613
- Landini, M., & Monsignori Fossi, B. C. 1990, *A&AS*, 82, 229

- Lemaire, P., Emerich, C., Vial, J., Curdt, W., Schühle, U., & Wilhelm, K. 2002, in ESA Special Publication, Vol. 508, From Solar Min to Max: Half a Solar Cycle with SOHO, ed. A. Wilson (Noordwijk: ESA), 219–222
- Lenz, D. D. 2004, *ApJ*, 604, 433
- Marocchi, D., Antonucci, E., & Giordano, S. 2001, *Annales Geophysicae*, 19, 135
- Mazzotta, P., Mazzitelli, G., Colafrancesco, S., & Vittorio, N. 1998, *A&AS*, 133, 403
- Morgan, H., Fineschi, S., Habbal, S. R., & Li, B. 2008, *A&A*, 482, 981
- Noci, G., Kohl, J. L., Antonucci, E., Tondello, G., Huber, M. C. E., Fineschi, S., Gardner, L. D., Naletto, G., Nicolosi, P., Raymond, J. C., Romoli, M., Spadaro, D., Siegmund, O. H. W., Benna, C., Ciaravella, A., Giordano, S., Michels, J., Modigliani, A., Panasyuk, A., Pernechele, C., Poletto, G., Smith, P. L., & Strachan, L. 1997, *Advances in Space Research*, 20, 2219
- Ofman, L. 2000, *Geophys. Res. Lett.*, 27, 2885
- . 2004, *Advances in Space Research*, 33, 681
- Ofman, L., Abbo, L., & Giordano, S. 2011, *ApJ*, 734, 30
- Ofman, L., & Kramar, M. 2010, in *Astronomical Society of the Pacific Conference Series*, Vol. 428, *Astronomical Society of the Pacific Conference Series*, ed. S. R. Cranmer, J. T. Hoeksema, & J. L. Kohl, 321–324
- Pneuman, G. W., & Kopp, R. A. 1971, *Sol. Phys.*, 18, 258
- Raymond, J. C., Kohl, J. L., Noci, G., Antonucci, E., Tondello, G., Huber, M. C. E., Gardner, L. D., Nicolosi, P., Fineschi, S., Romoli, M., Spadaro, D., Siegmund, O. H. W., Benna, C., Ciaravella, A., Cranmer, S., Giordano, S., Karovska, M.,

- Martin, R., Michels, J., Modigliani, A., Naletto, G., Panasyuk, A., Pernechele, C., Poletto, G., Smith, P. L., Suleiman, R. M., & Strachan, L. 1997, *Sol. Phys.*, 175, 645
- Steinolfson, R. S., & Nakagawa, Y. 1976, *ApJ*, 207, 300
- Strachan, L., Suleiman, R., Panasyuk, A. V., Biesecker, D. A., & Kohl, J. L. 2002, *ApJ*, 571, 1008
- Uzzo, M., Ko, Y., Raymond, J. C., Wurz, P., & Ipavich, F. M. 2003, *ApJ*, 585, 1062
- Uzzo, M., Ko, Y.-K., & Raymond, J. C. 2004, *ApJ*, 603, 760
- Uzzo, M., Strachan, L., & Vourlidas, A. 2007, *ApJ*, 671, 912
- Uzzo, M., Strachan, L., Vourlidas, A., Ko, Y.-K., & Raymond, J. C. 2006, *ApJ*, 645, 720
- Vásquez, A. M., & Raymond, J. C. 2005, *ApJ*, 619, 1132
- Withbroe, G. L., Kohl, J. L., Weiser, H., & Munro, R. H. 1982, *Space Sci. Rev.*, 33, 17
- Zangrilli, L., Poletto, G., Biesecker, D., & Raymond, J. C. 2001, in *American Institute of Physics Conference Series*, Vol. 598, Joint SOHO/ACE workshop "Solar and Galactic Composition", ed. R. F. Wimmer-Schweingruber, 71–76

Table 1: The most probable velocity $V_{1/e}$, and the corresponding kinetic temperatures $T_{k,i}$ of Mg x and O vi lines observed in quiescent streamers by UVCS.

Height R_{\odot}	Date YY.MM.DD.hh	Slit μm	$V_{1/e,MgX}$ km/s	$T_{k,MgX}$ MK	$V_{1/e,OVI}$ km/s	$T_{k,OVI}$ MK
1.39	96.08.16.17	31	60 ± 13	5.2 ± 2.3	50 ± 5	2.4 ± 0.5
1.49	96.07.15.18	76	71 ± 7	7.3 ± 1.4	70 ± 3	4.8 ± 0.4
1.61	97.07.31.19	100	72 ± 8	7.5 ± 1.7	58 ± 3	3.3 ± 0.3
1.70	96.07.23.16	97	70 ± 7	7.1 ± 1.4	63 ± 3	3.9 ± 0.4

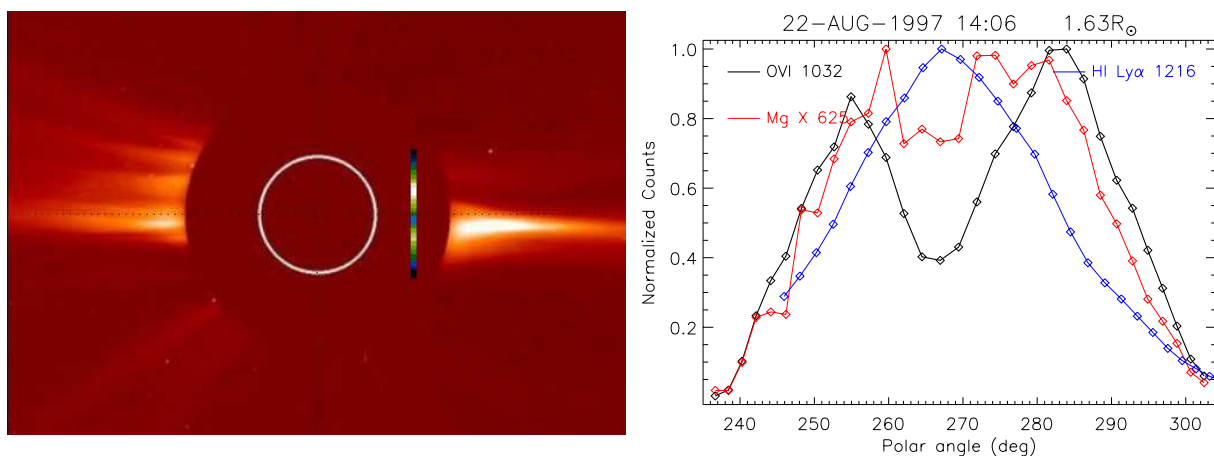


Fig. 1.— Quiescent streamer observation at solar minimum in visible light and UV performed on August 22, 1997. Left panel: White light image from LASCO C2 with superimposed the O VI 1032Å intensity image along UVCS slit. Right panel: Intensity profiles along the instrumental slit at $1.63 R_{\odot}$ of H I Ly α (blue), O VI 1032Å (black) and Mg X 625Å (red) spectral lines.

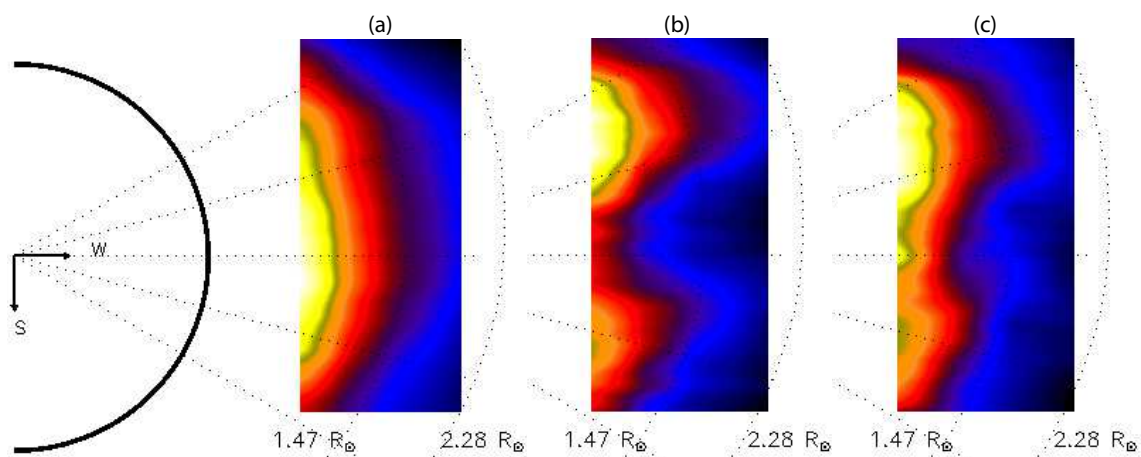


Fig. 2.— Streamer intensity images from 1.47 to $2.28 R_{\odot}$, as observed by UVCS on Sep. 26, 1997, in (a) H I Ly α (b) O VI 1032Å, and (c) Mg X 625Å. The left panel shows the corresponding solar coordinates.

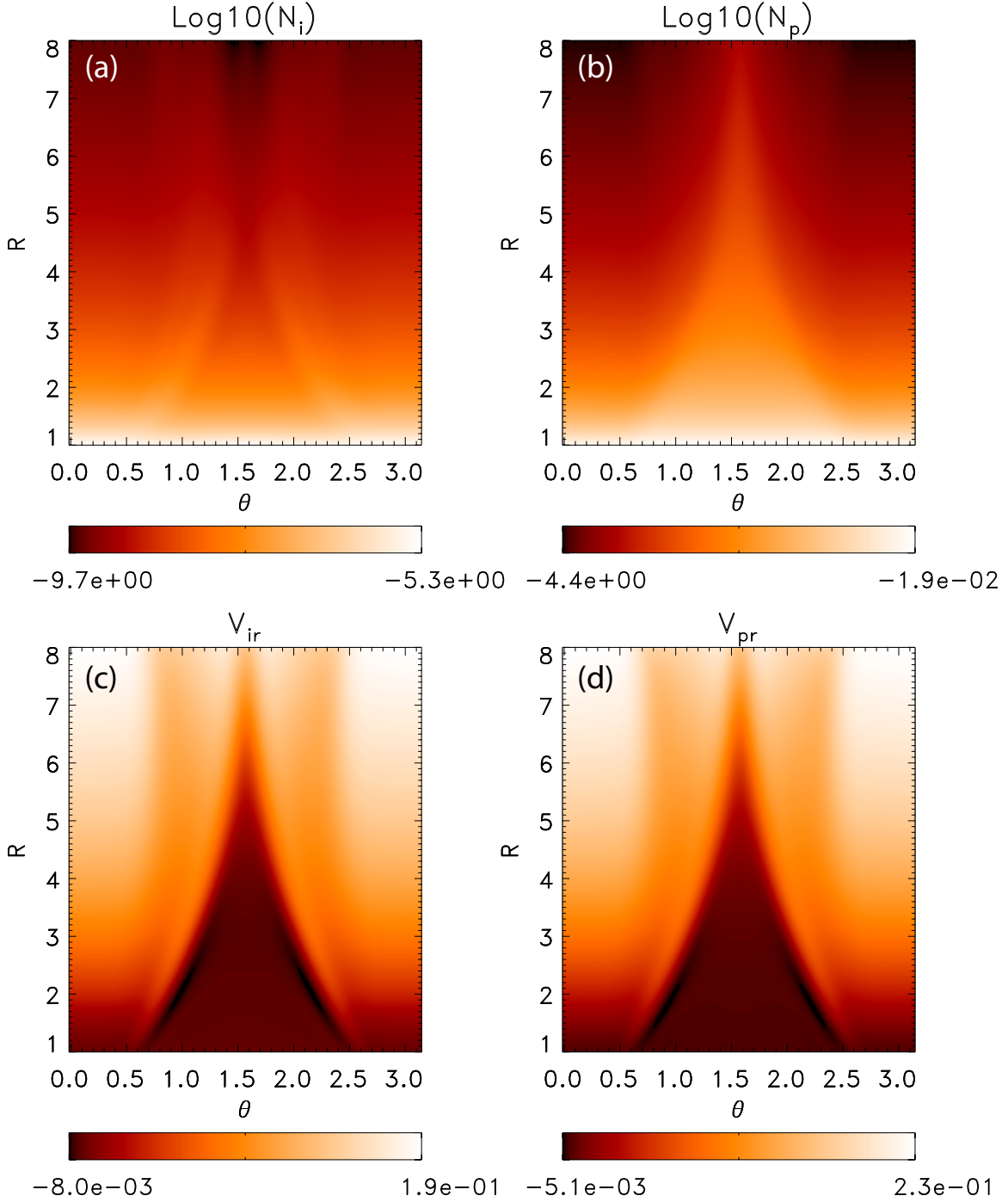


Fig. 3.— The density of (a) protons, and (b) Mg^{9+} ions in the streamer calculated with the three-fluid model at $t = 98.1\tau_A$. The corresponding radial velocity V_r in units of V_A of (c) protons, and (d) Mg^{9+} ions. The animation of the Mg^{9+} density is available in the electronic version of this article.

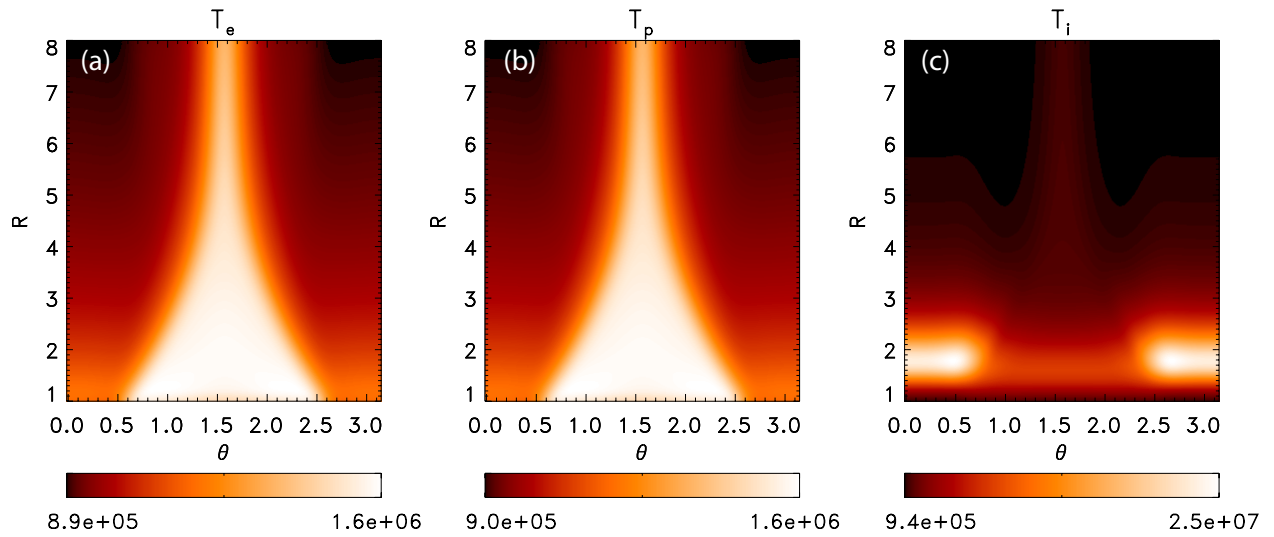


Fig. 4.— The kinetic temperature maps of (a) electrons , (b) protons, and (c) Mg^{9+} ions in the streamer calculated with the three-fluid model at $t = 98.1\tau_A$.

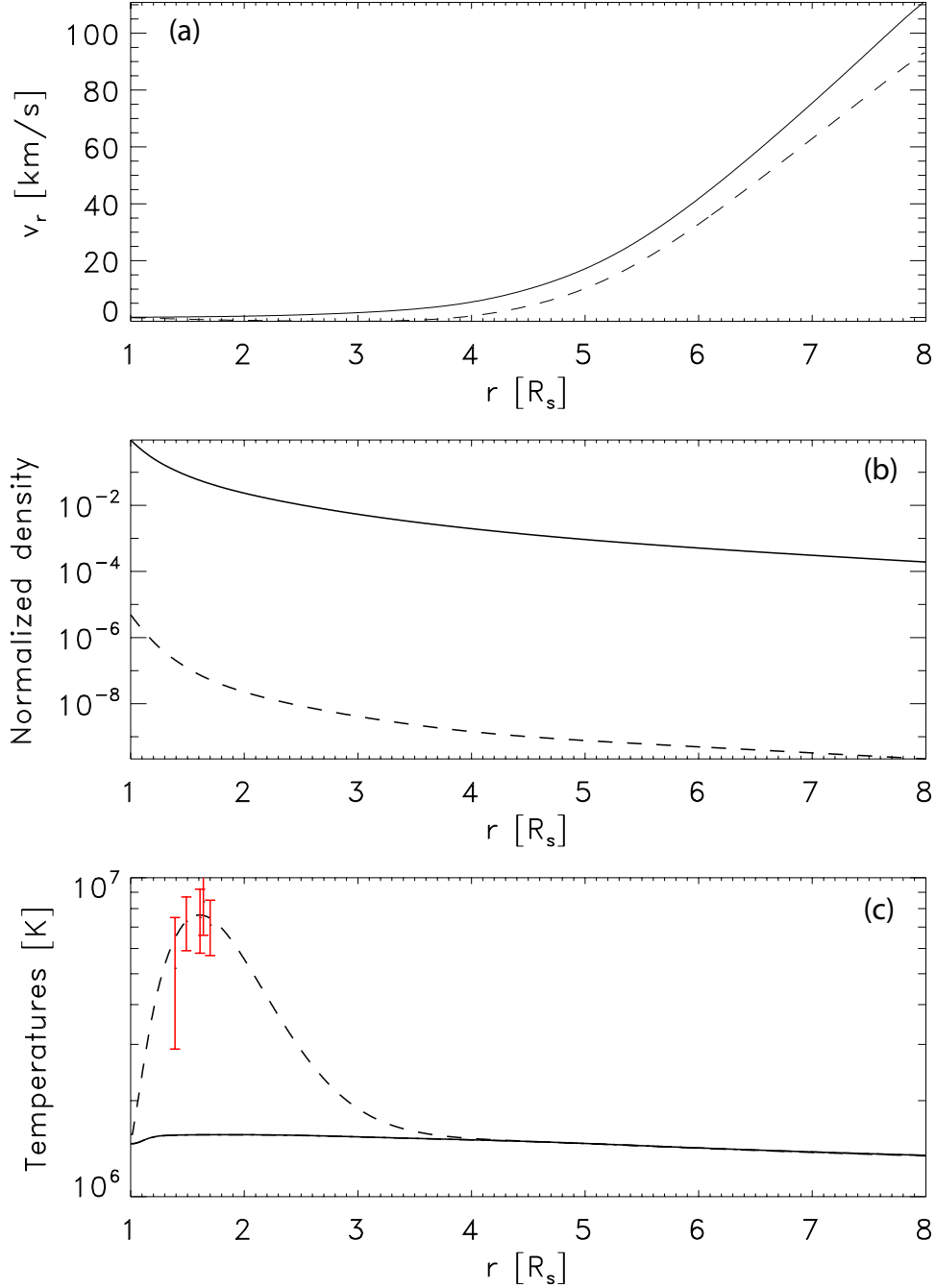


Fig. 5.— The cross-section in the radial direction at the center of the streamer calculated with the three-fluid model at $t = 98.1\tau_A$ (protons - solid; Mg^{9+} ions - dashes). (a) The radial velocity. (b) The normalized density. (c) The temperature (electrons shown with dotted curve that overlaps the proton temperature). The red symbols with error bars show the kinetic temperatures of Mg^{9+} given in Table 1.

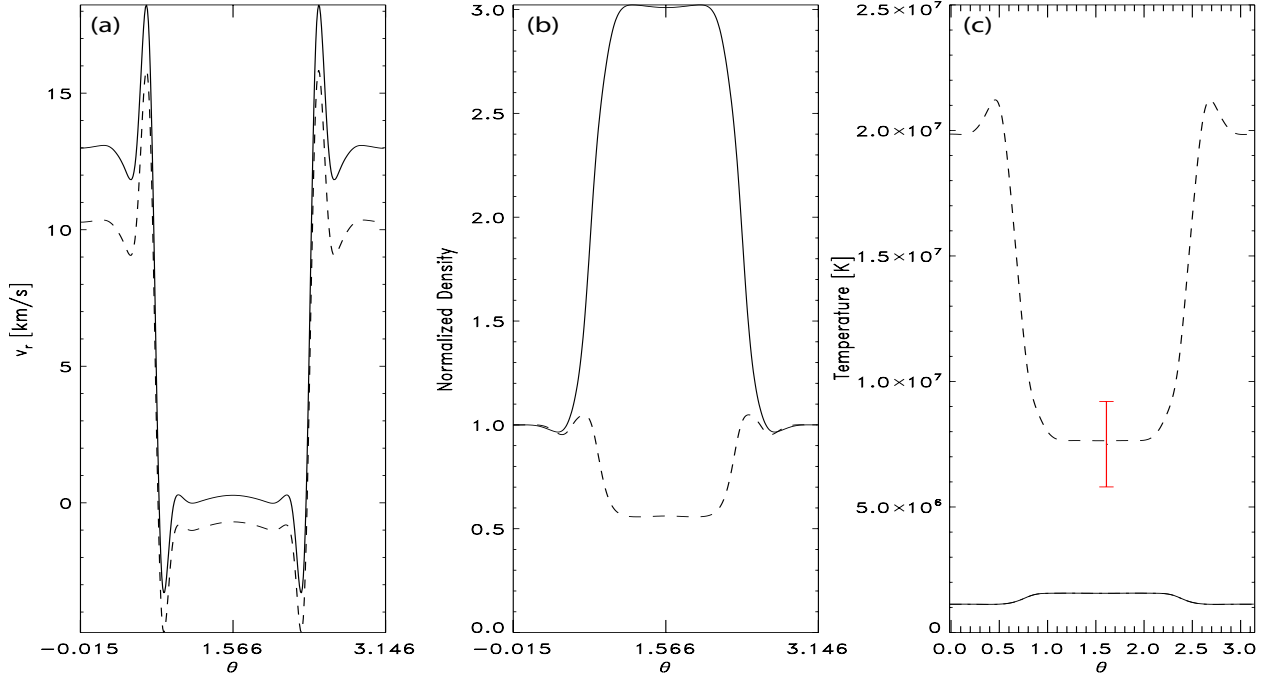


Fig. 6.— The cross-section in the latitudinal (θ) direction at $r = 1.61 R_{\odot}$ of the streamer calculated with the three-fluid model at $t = 98.1\tau_A$ (protons - solid; Mg^{9+} ions - dashes). (a) The radial velocity. (b) The normalized density. (c) The temperature (electrons shown with dotted curve that overlaps the proton temperature). The red symbol with the error bar shows the Mg^{9+} kinetic temperature at $r = 1.61 R_{\odot}$ given in Table 1.

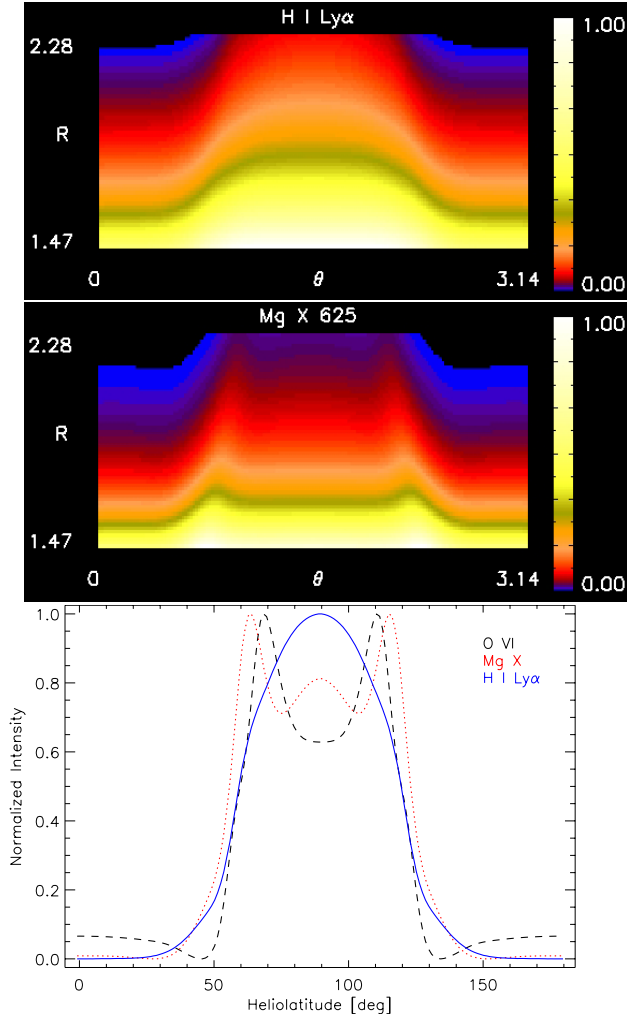


Fig. 7.— The normalized intensity maps of H I Ly α (top) and of Mg X (middle) lines as computed from the model. The latitudinal intensity profiles at $1.63 R_{\odot}$ are shown in the bottom panel (H I, solid blue line; Mg X, dotted red line, O VI, dashed black line).

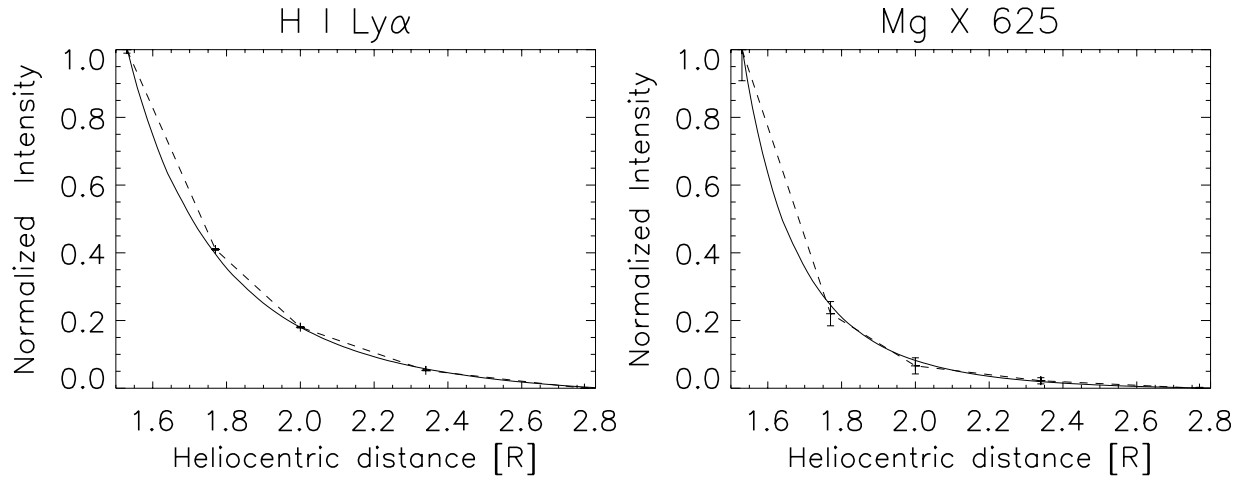


Fig. 8.— The radial intensity profiles (normalized) from 1.5 to 2.8 R_{\odot} for H I Ly α (left) and of Mg X (right) lines. The solid line shows the values computed from the model, the points and the dashed line are the values observed by UVCS.